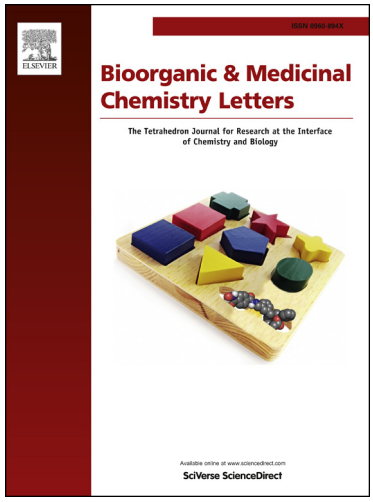

In silico to *in vitro* screening of hydroxypyridinones as acetylcholinesterase inhibitors

Maria A. Telpoukhovskaia, Brian O. Patrick, Cristina Rodríguez-Rodríguez, Chris Orvig

PII: S0960-894X(16)30094-4
DOI: http://dx.doi.org/10.1016/j.bmcl.2016.01.080
Reference: BMCL 23545

To appear in: *Bioorganic & Medicinal Chemistry Letters*

Received Date: 8 December 2015
Revised Date: 26 January 2016
Accepted Date: 29 January 2016

Please cite this article as: Telpoukhovskaia, M.A., Patrick, B.O., Rodríguez-Rodríguez, C., Orvig, C., *In silico* to *in vitro* screening of hydroxypyridinones as acetylcholinesterase inhibitors, *Bioorganic & Medicinal Chemistry Letters* (2016), doi: http://dx.doi.org/10.1016/j.bmcl.2016.01.080

Graphical Abstract

***In silico* to *in vitro* screening of hydroxypyridinones as acetylcholinesterase inhibitors**

Leave this area blank for abstract info.

Maria A. Telpoukhovskaia, Brian O. Patrick, Cristina Rodríguez-Rodríguez* and Chris Orvig*

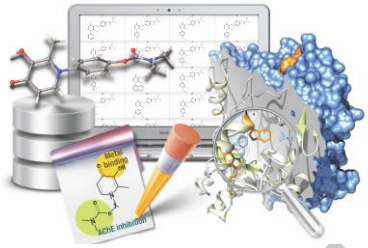

Bioorganic & Medicinal Chemistry Letters
journal homepage: www.elsevier.com

In silico to *in vitro* screening of hydroxypyridinones as acetylcholinesterase inhibitors

Maria A. Telpoukhovskaia,[†] Brian O. Patrick, Cristina Rodríguez-Rodríguez[‡*] and Chris Orvig[*]

Medicinal Inorganic Chemistry Group, Department of Chemistry, University of British Columbia, 2036 Main Mall, Vancouver, BC, V6T 1Z1, Canada

ARTICLE INFO

Article history:
Received
Revised
Accepted
Available online

Keywords:
hydroxypyridinone
dimethylcarbamate
acetylcholinesterase
inhibitor
virtual library screening

ABSTRACT

We have previously shown the improved acetylcholinesterase inhibitory activity of a model hydroxypyridinone compound transforming the hydroxyl group on the main ring into an *N,N*-dimethylcarbamate group; in the course of that study we developed a computational model to screen compounds for enzymatic activity. Herein we report development of second generation libraries. Candidates that adhere to drug-like criteria from a virtual library of compounds were tested using computational docking studies. Synthesis and characterization of chosen test compounds and their acetylcholinesterase inhibitory activity are presented.

Curing Alzheimer's disease (AD) remains an elusive therapeutic goal, while the number of patients who get the bleak prognosis increases with the rise in life expectancy.[1] The formulation of the amyloid cascade hypothesis, which states that the deposits of the protein amyloid-beta are the key in AD development, has contributed to establishing many research avenues, the outcomes of which have been tested in clinical trials; unfortunately, it has yet to yield a successful treatment.[2] Other related areas of research include studies with antioxidant compounds[3] and metal chelators such as the drug PBT2 (5,7-dichloro-2-((dimethylamino)-methyl)-8-hydroxyquinoline), which is under investigation in clinical trials.[4] With the success of this ligand in preclinical studies, and taking into account the multifactorial nature of AD, chelators that possess antioxidant and/or amyloid-beta binding functionalities are being explored within the medicinal inorganic chemistry community.[5]

Our group takes advantage of the versatility of the hydroxypyridinone (HPO) family in three ways – its promiscuity toward metals (by acting as a binder in different stoichiometries), its ability to accommodate various *N*-substituents without influencing metal binding activity, as well as the ability to be transformed into a prodrug through installation of a masking group onto the hydroxyl group. For instance, the chelation of **Hppp** (Fig. 1) has been studied with Cu,[6] Zn,[7] Fe,[7] Al(III),[8] In(III),[8] and Ga(III)[8] in the solid states. **Hhpp** is a close relative of **Hppp**, with a hydroxyl group off the phenyl *N*-substituent of the HPO ring (Fig. 1), and we have studied Ga(III) chelation to the glucose conjugate of **Hhpp** on the phenyl substituent.[9] In fact, this molecular scaffold has attracted many investigators to develop radiopharmaceuticals for diagnostic imaging and radiotherapy; for example, HPO ligands able to coordinate ^{67}Ga and ^{68}Ga have been investigated *in vivo*.[10,11] On the other hand, the benefits of incorporating a glucose in the molecular structure (for brain uptake and cytotoxicity considerations) have also been investigated by conjugation to hydroxyl of HPO ring; for instance, rat brain uptake of ^{125}I radiolabeled glycosylated **Hppp** analogue was investigated.[12]

With the observation that the neurotransmitter acetylcholine is depleted in patients suffering from AD due to loss of cholinergic neurons came a strategy for their treatment. Drugs such as rivastigmine (Fig. 1), tacrine, donepezil, and galantamine act as acetylcholine esterase inhibitors, essentially increasing the amount of acetylcholine by blocking its breakdown.[13] While this strategy only works in less than half of the patients for a couple of years,[14] ameliorative treatment remains the only option in the clinic.[13] The mode of action of these drugs remains in their ability to interact within the active site of the AChE enzyme: tacrine acts without altering the structure of the enzyme (reversible

[*] Corresponding author. Tel.: +1-604-827-1833; fax: +1-604-822-7894; e-mail: cristina.rodriguez@ubc.ca
[*] Corresponding author. Tel.: +1-604-822-4449; fax: +1-604-822-2847; e-mail: orvig@chem.ubc.ca
[†] Present address: Gladstone Institute of Neurological Disease, 1650 Owens Street, San Francisco, CA, 94158, USA.
[‡] Present address: Department of Physics & Astronomy, University of British Columbia, 6224 Agricultural Road, Vancouver, BC, V6T 1Z1, Canada.

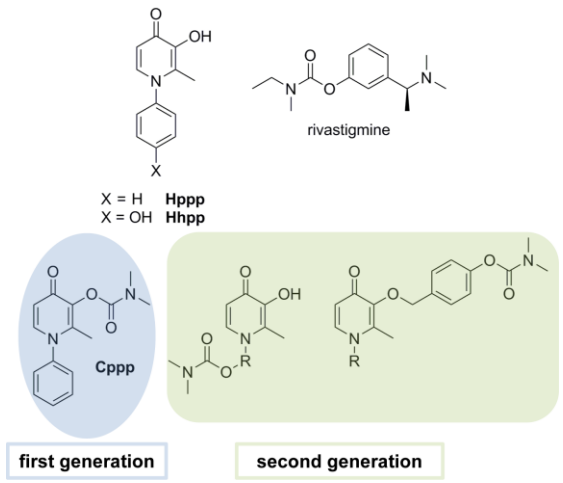

Fig. 1 Top: HPO pro-ligands **Hppp** and **Hhpp**, neurotransmitter acetylcholine. Bottom: the first generation compound (**Cppp**), as well as two second generation designs.

inhibitor),[15] while rivastigmine permanently modifies it.[16] Notably, the aftermath of the inhibition has been crystallized, and solid state structure analysis reveals that the carbamoyl group of the drug is covalently attached to the enzyme, with the rest of rivastigmine in the catalytic site with the phenol functional group exposed.[16]

Following a previously reported strategy that imbues a metal chelate with acetylcholinesterase inhibitory activity,[17] we functionalized **Hppp** with dimethyl carbamate to yield **Cppp** (Fig. 1).[18] We found that the acetylcholinesterase inhibitory activity of **Cppp** (Fig. 1) is improved compared to the parent compound **Hppp** and through kinetic studies we determined that **Cppp** is a reversible inhibitor.[18] The computational studies illustrated how the compound interacts with the enzyme to achieve the observed activity.[18] Because it acts as a reversible inhibitor, the metal chelating functionality is not accessible for **Cppp**.

The new approach detailed in this work consists of two modifications to conserve the metal chelating core of the HPO scaffold. In the first approach, the metal binding site is left intact and the carbamate is moved to be positioned on the *N*-substituent of the HPO (Fig. 1). In the second approach, the carbamate is attached to the HPO ring by the benzyl ether linker spacer (Fig. 1) that had been shown by Cohen and coworkers to be eliminated upon enzymatic removal of an acetyl group.[19] Based on these designs, we created a virtual library consisting of 80 compounds. After filtering out unsuitable candidates, we performed docking studies and chose three model compounds **Chpp, Cchpp,** and **Cbppp** (derivatives of **Hppp** and **Hhpp)** to synthesize and perform *in vitro* acetylcholinesterase inhibitory activity studies. Overall, we aim to continue the development of the multifunctional HPO scaffold by exploring its novel inhibitory functionality with the aid of computational studies.

In the first step to create a virtual library of molecules, SciFinder was consulted to compile a pool of HPOs that had been synthesized and characterized. In the next step, the *N*,*N*-dimethyl carbamate was attached to either the main ring of the HPO with a benzyl ether linker, or to the N-substituent (Fig. 1). This resulted in a virtual database of 80 molecules total, with 40 in each half of the library (Figs. S1 and S2).

The initial database was prefiltered to create a smaller database that captures the diversity of the entire set, while reducing the computational demands of the virtual screening process. In the first stage, the database was filtered to discard those molecules deemed unlikely to be suitable drug candidates according to Lipinski's parameters.[20] Lipinski's rules are some of the guiding parameters that researchers use to filter out potentially problematic compounds: molecules were selected for low molecular weight (under 500), appropriate lipophilicity (with logP under 5), low number of hydrogen acceptor (under 10) and donor (under 5) atoms. Subsequently, the parameter log BB was calculated with Clark's equation (eqn 1) incorporating parameters calculated using the online chemoinformatics software molinspiration (http://www.molinspiration.com), which approximates LogP with miLogP value.

$$\log BB = - 0.0148\ TPSA + 0.152\ clogP + 0.139 \qquad (1)$$

Log BB is a way to predict passive permeability of compounds through the BBB, which takes into account topological polar surface area (TPSA) and octanol-water partition

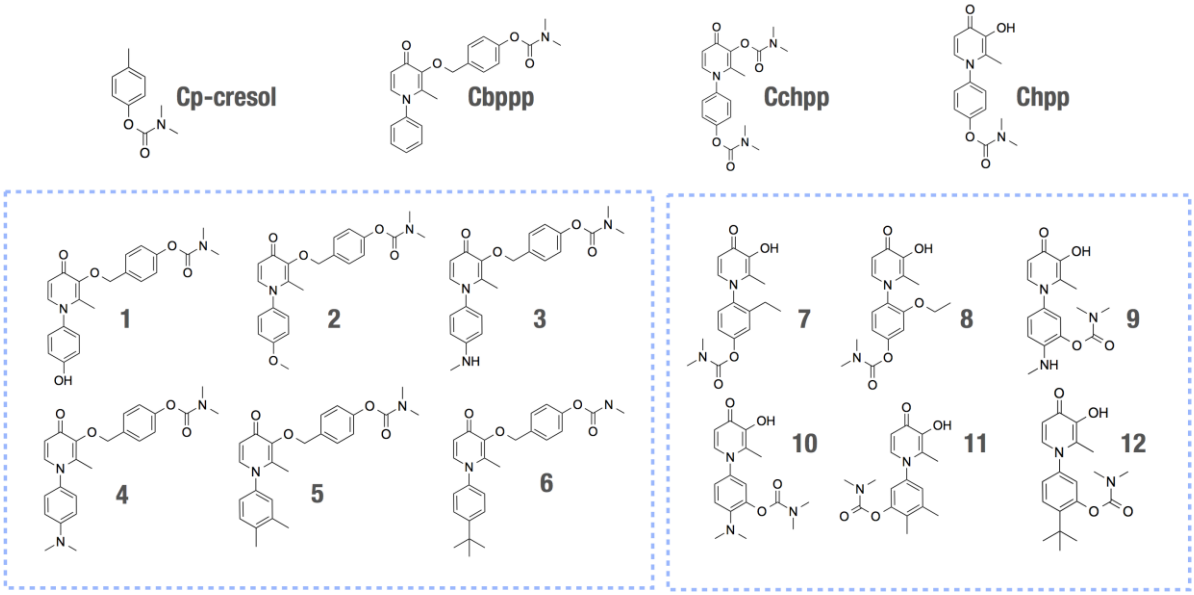

Fig. 2 Selected compounds for computational docking analysis.

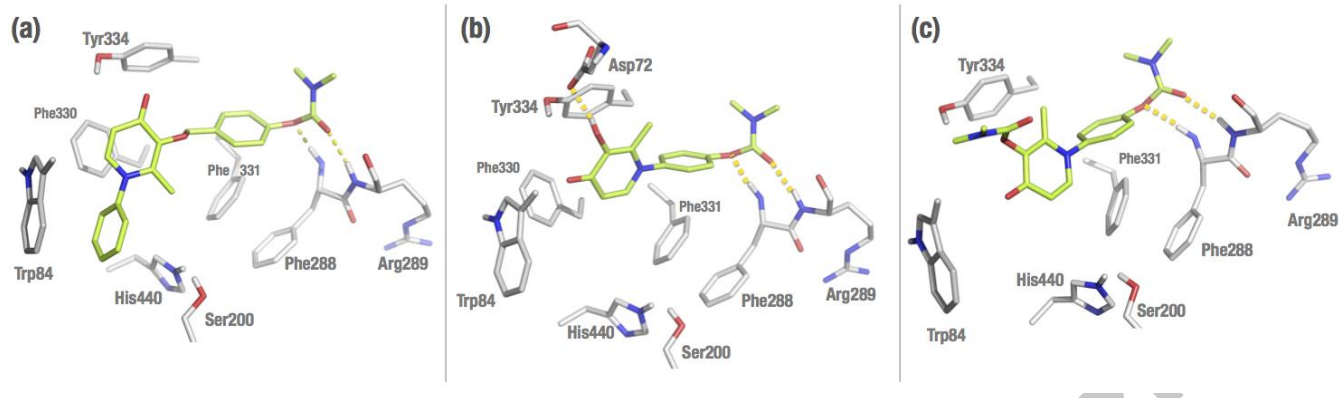

Fig. 3 Top-scored docking poses for the lead compounds a) **Cbppp**, b) **Chpp**, and c) **Cchpp**, in *Tc*AChE.

coefficient (logP), one measure of lipophilicity. Compounds with logBB < -1 were discarded.[21] As well, compounds containing reactive functional groups (like aliphatic ketones and aliphatic esters) were removed from the library due to their instability in serum and reactivity toward proteins and other biomolecules.[22]

As a result of this filtering process, we obtained 59 molecules, from which 15 structurally diverse compounds were selected for an in-depth molecular docking analysis in order to understand the mode of interaction with the AChE enzyme (Fig. 2). Structure-based molecular docking analysis has been used for rationalizing ligand-AChE interactions and understanding the observed inhibitory activity.[23–25] Molecular modeling using the 3D crystallographic structure of AChE from *Torpedo californica* (*Tc*AChE) co-crystallized with tacrine (PDB 1ACJ) as a receptor was performed, as detailed in our previously published work.[18] Note that the *in vitro* assays were performed using the Electric eel AChE; a comparative sequence analysis of both enzymes shows a high degree of amino acids conservation as shown in Fig. S3. Thus, we can consider the active site very similar in both enzymes. The binding site of *Tc*AChE revealed a narrow and deep cavity lined by aromatic side chains. The dynamic motion of Phe330 and Trp279 residues is apparent after analysing the several available crystal structures of AChE bound to different ligands. Therefore, a molecular docking protocol was performed allowing random rotation of Phe330 and Trp279 as validated previously with tacrine and a first generation of carbamoyl-derivatized HPO.[18] An open conformation of Phe330 on binding of the *Tc*AChE with rivastigmine was reported in its X-ray structure (PDB code 1GQR). In this work, according to docking studies, Phe330 also adopts an open conformation when the studied compounds bind to *Tc*AChE.

Molecular docking analysis was performed on the 15 HPO molecules (Fig. 2) that were obtained as a result of the virtual screening process. For each molecule, the top-scored pose (lowest binding energy) in the most stable cluster was considered as the most favourable docking conformation (Figs. 3 and S4). According to docking results, each molecule interacts with *Tc*AChE via hydrogen bonding and π-stacking, with locations in both the peripheral and the active sites. Due to their molecular similarity, the binding of molecules to AChE present common patterns (Figs. 3 and S4). In most cases, the interaction is between with the carbamate moiety of the molecules and the backbone formed by the amino acids Phe288 and Arg289 at a bond length of ~ 2.0 Å in the acyl pocket of the enzyme. In other cases, π-π stacking interactions are observed with aromatic residues e.g. Phe330 and Trp84 (**Cbppp** and 1) or Tyr334 (9) (Figs. 3 and S4) located in the anionic, and the peripheral sites. Some of these molecules, particularly 4, 5, and 6 show two hydrogen bonds between Ser200 and His440 and the carbonyl oxygen of the pyridinone scaffold (Fig. S4) stabilizing the carbamate moiety far from the catalytic site and therefore blocking any possible hydrolysis reaction. Overall, after this analysis we conclude that all these inhibitors should act in a reversible manner.

Further analysis was performed on **Cbppp**, **Cchpp,** and **Chpp**. As stated before, the main differences between them are the number of carbamate motifs and their position. Molecular docking simulations predicted that **Cbppp**, **Cchpp,** and **Chpp** present similar interactions and conformations (Fig. 3). In terms of ligand-receptor interactions, the HPO scaffold does not participate as an active group to guide the molecule inside the active site of the AChE. On the contrary, the presence of **Cp-cresol** motif is responsible for the interaction in the acyl pocket forming hydrogen bonds with the amide groups (NH) of the backbone of the enzyme (Phe288 and Arg289) (Fig. 3). This interaction may prevent the compounds from going into the catalytic triad.

Among all docking conformations, **Cbppp** had the best docking score of -5.59 kcal/mol, followed by compounds **Cchpp** and **Chpp** with predicted binding affinities of -5.31 and -4.96 kcal/mol, respectively. **Cbppp** was found to form two favourable π-π stacking interactions: (i) between the phenyl ring of **Cbppp** and the indole ring of Trp84; and (ii) the HPO scaffold and the Phe330 amino acid both at the anionic site of AChE (Fig. 3). Similarly, docking simulations revealed that the best-scored docking conformation for **Cchpp** showed a binding pattern very similar to that of **Cbppp** (Fig. 3); however, the π- π stacking interactions were not observed (Fig. 3). **Chpp** showed an additional hydrogen bonding interaction with Asp72 (Fig. 3). In order to study which part of the molecule is responsible for the observed inhibition, we performed docking and experimental analysis of **Cp-cresol** (Fig. 2). In all the poses obtained from docking, **Cp-cresol** shows interactions with the aforementioned amino acids in the acyl pocket (Phe288 and Arg289), thus we assume that it is unlikely that this motif is responsible for the difference in observed binding affinity. The trend of ligand affinity has good correlation with the experimental *in vitro* results, as detailed below.

As a conclusion, based on the most stable conformations, we predict that the interactions observed with molecular docking calculations lead to reversible AChE inhibitors. The best interaction is shown for those molecules from the library of compounds in which the carbamate moiety is positioned on the HPO ring using a spacer. Interestingly, the presence of two carbamate motifs in the molecule does not result in improved interaction. When all docking results were analyzed, a few conformations close to the active site of *Tc*AChE (His440,

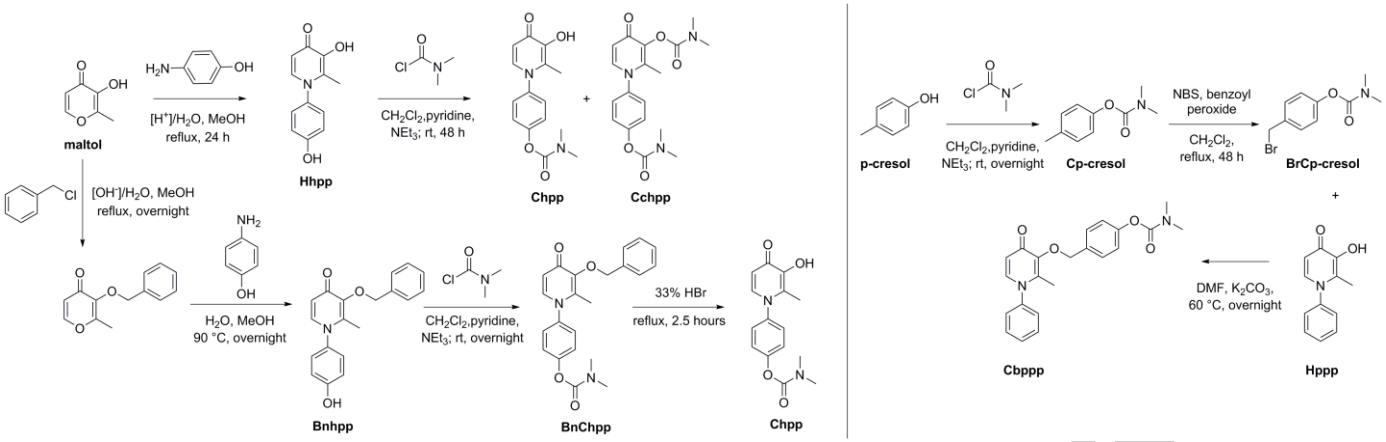

Scheme 1 Left: Synthetic routes for **Chpp**. Right: Synthetic route for **Cbppp**.

Ser200 and Glu327) for compounds **Cbppp**, **Chpp**, and **Cchpp** were observed. We set out to test these molecules *in vitro* and to assess their inhibition mode with acetylcholinesterase.

Synthesis of compound **Chpp** followed the synthetic routes in Scheme 1. The product could be obtained using two routes. In the first, **Hhpp** is reacted with *N*,*N*-dimethylcarbamoyl chloride,[18] resulting in both singly and doubly carbamated compounds, **Chpp** and **Cchpp**, that were separated by column chromatography. The second route avoids the doubly carbamated by-product by starting with a benzyl protected starting material, **Bnhpp.** After carbamation, **BnChpp** must be debenzylated, and while both these routes result in **Chpp**, the second requires two extra steps. Identity and purity of **Chpp** and **Cchpp** were established with ^{1}H, ^{13}C NMR spectroscopies (Figs. S5-8), HRMS, and EA. Starting materials **Hhpp** and **Bnhpp**, as well as **Chpp** were analyzed by X-ray crystallography and their solid state structures appear in Fig. S9. Crystal refinement data and selected bonds and angles can be found in Tables S1 and S2. As can be seen from Table S2, HPO ring retains its bond distances across the three compounds.

Compound **Cbppp** was synthesized using the route in Scheme 1. First, p-cresol is carbamated[18] and brominated using NBS,[19] and then it is reacted[19] with **Hppp**. The product was characterized by ^{1}H and ^{13}C NMR spectroscopies (Figs. S10 and S11) and HRMS, and HPLC was used to provide an assessment of its purity (Fig. S12).

The synthetic intermediate **Cp-cresol** was of particular interest as it is a fragment of the final products **Cbppp** and **Chpp**. Since we aimed to include this compound in *in vitro* and computational studies, we characterized it fully by ^{1}H, ^{13}C NMR spectroscopies (Figs. S13 and S14), HRMS, and EA. As well, a single crystal of **Cp-cresol** was studied by X-ray crystallography (Table S3, Fig. S9) to reveal the expected delocalization of the electrons from the C8-O2 double bond to result in shortening of C8-N1 bond (1.35 Å compared to 1.45 Å for the N1-C10 and N1-C9 bonds), giving it partial double bond character. One of the *N*-methyl groups is nearly planar, with the torsion angle of -1.5° for O2-C8-N1-C10, while the other methyl group is out of the plane by 10°. The partial double bond character translates into the inability of the C8-N1 bond to rotate at room temperature, resulting in inequivalent N-methyl groups that are observed with NMR spectroscopy (Figs. S13 and S14).

In vitro acetylcholinesterase activity was established for the synthesized compounds **Chpp**, **Cchpp**, **Cbppp**, as well as for the fragment **Cp-cresol** (Figs S15 and S16). As can be seen in Figure 4, all compounds have similar acetylcholinesterase inhibitory activity: 219.9 μM (**Hppp**), 347.6 μM (**Chpp**), 252.3 μM (**Cchpp**), and 216.5 μM (**Cbppp**). It was also noted that the carbamated fragment **Cp-cresol** has inhibitory activity that is about one order of magnitude less: 1282 μM.

To investigate the mode of action of these inhibitors, substrate turnover (of acetylthiocholine iodide, ATCI) was monitored over 60 minutes. We determined that compared to control (no inhibitor present), the compounds **Chpp** and **Cbppp** presented similar profiles – that is, the turnover rate remained nearly constant over time (Fig. 4). This profile is similar to what we observed with previous generation compound, **Cppp**, as well as reference compound tacrine that is a well-known reversible inhibitor.[18]

Another piece of evidence suggesting that the inhibition observed from **Chpp** and **Cbppp** is reversible is based on analysing drug activation extracts by mass spectrometry and TLC. Solely peaks corresponding to masses of and bands of **Chpp** and **Cbppp** were observed after 1 or 24 hours of incubation with AChE. In another set of experiments, dilute $Fe(ClO_4)_3$ was added to reaction vials with AChE and **Chpp** or **Cbppp**. Consistent with previous results, no metal chelation to **Cbppp** was observed. On the other hand, the advantage of **Chpp** – in that it retains metal chelation became apparent as a **Chpp**:iron complex was observed by mass spectrometry.

In conclusion, a virtual library for a second generation of carbamated HPOs was prepared following two different strategies: (i) inserting a linker between the carbamate and the HPO and (ii) positioning the carbamate moiety on the *N*-substituent of the HPO. After pre-filtering the initial database, we selected 15 compounds to study by molecular docking. Molecular docking studies provided valuable insight into the

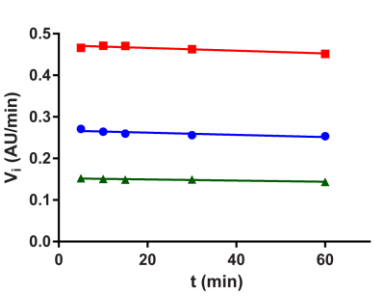

	IC_{50} (μM)
Hppp	219.9
Chpp	347.6
Cchpp	252.3
Cbppp	216.5
Cp-cresol	1282
tacrine	0.002
rivastigmine[26]	5.5
Cppp[18]	48.8
control	

Fig. 4 Left: Inhibition kinetics of **Chpp** (blue) and **Cbppp** (green) with *eel*AChE: enzymatic activity vs. time, as compared to a control with no inhibitor (red). Right: Table of IC_{50} values for *in vitro eel*AChE activity for **Hppp**, **Chph**, **Cchpp**, **Cbppp**, **Cp-cresol**, tacrine, rivastigmine, and **Cppp**.

activity of the second generation of carbamated HPO derivatives. It was revealed that the compounds interact in such a way that prohibits them from entering the active site, which is why the inhibitory action is reversible. Therefore, in cases where metal binding is advantageous, an HPO such as **Chpp** with an unmasked metal chelating site can be used. **Cbppp, Chpp**, and **Cchpp** were synthesised, and their identities and purities were established with ^{1}H and ^{13}C NMR spectroscopy, HRMS, and EA, as well as X-ray crystallography studies for **Chpp**. It was then confirmed experimentally that these compounds act as reversible inhibitors of AChE. Acetylcholinesterase inhibition is currently one of the only ways to help Alzheimer's disease patients with memory problems. HPOs such as **Chpp** can act as both metal binders and AChE inhibitors, thus combining two potentially important aspects of AD therapy in one compound.

Acknowledgments

We thank the Alzheimer Society of Canada for a doctoral award (M.A.T.), the Natural Sciences and Engineering Research Council of Canada (NSERC) for a Discovery Grant (C.O.) and a PGSD-2 award (M.A.T.), and the Canadian Institutes of Health Research (CIHR) Proof of Principle program (C.O.). C.O. acknowledges the Canada Council for the Arts for a Killam Research Fellowship (2011-2013) and the Alexander von Humboldt Foundation for a Forschungspreis. As well, we thank Agència de Gestió d'Ajuts Universitaris i de Recerca (AGAUR) from Generalitat de Catalunya (Beatriu de Pinós (BP-DGR-2009)) for postdoctoral fellowship funding (C.R.R.), and the staff of UBC Chemistry analytical services for help with characterization of compounds. Finally, we thank Caterina Ramogida for analysis of compounds by HPLC.

Supplementary Data

Supplementary data (Figs. S1-S16, Tables S1-S3, and X-ray crystal data in CIF format) associated with this article can be found, in the online version, at http://dx.doi.org/10.1016/ j.bmcl.0000.00.000. Crystallographic data for **Hhpp**, **Bnhpp**, **Chpp**, and **Cp-cresol** can be found free of charge at http://www.ccdc.cam.ac.uk from the Cambridge Crystallographic Data Centre (CCDC 988955-988958, respectively).

References and notes

1. N. L. Batsch, and M. S. Mittelman, *Overcoming the stigma of dementia: World Alzheimer Report 2012*, accessed 29 November 2015, https://www.alz.org/documents_custom/world_report_2012_final.pdf.
2. Palmer, A. M. *Drug Discovery Today* **2012**, *17*, 1157.
3. Shinto, L.; Quinn, J.; Montine, T.; Dodge, H. H.; Woodward, W.; Baldauf-Wagner, S.; Waichunas, D.; Bumgarner, L.; Bourdette, D.; Silbert, L.; Kaye, J. *J. Alzheimers Dis.* **2014**, *38*, 111.
4. Prana Biotechnology announces top line results of Phase 2 IMAGINE trial of PBT2 in Alzheimer's disease, 2014, media release, accessed 29 November 2015, http://pranabio.com/news/prana-biotechnology-announces-top-line-results-phase-2-imagine-trial-pbt2-alzheimers-disease.
5. Perez, L. R.; Franz, K. J. *J. Chem. Soc., Dalton Trans.* **2010**, *39*, 2177.
6. Scott, L. E.; Page, B. D. G.; Patrick, B. O.; Orvig, C. *J. Chem. Soc., Dalton Trans.* **2008**, 6364.
7. Telpoukhovskaia, M. A.; Rodríguez-Rodríguez, C.; Scott, L. E.; Page, B. D. G.; Patrick, B. O.; Orvig, C. *J. Inorg. Biochem.* **2014**, *132*, 59.
8. Zhang, Z.; Rettig, S. J.; Orvig, C. *Inorg. Chem.* **1991**, *30*, 509.
9. Green, D. E.; Ferreira, C. L.; Stick, R. V.; Patrick, B. O.; Adam, M. J.; Orvig, C. *Bioconjugate Chem.* **2005**, *16*, 1597.
10. Chaves, S.; Mendonça, A. C.; Marques, S. M.; Prata, M. I.; Santos, A. C.; Martins, A. F.; Geraldes, C. F. G. C.; Santos, M. A. *J. Inorg. Biochem.* **2011**, *105*, 31.
11. Ma, M. T.; Cullinane, C.; Imberti, C.; Baguña Torres, J.; Terry, S. Y. A.; Roselt, P.; Hicks, R. J.; Blower, P. J. *Bioconjugate Chem.* **2015**, DOI: 10.1021/acs.bioconjchem.5b00335.
12. Schugar, H.; Green, D. E.; Bowen, M. L.; Scott, L. E.; Storr, T.; Böhmerle, K.; Thomas, F.; Allen, D. D.; Lockman, P. R.; Merkel, M.; Thompson, K. H.; Orvig, C. *Angew. Chem. Int. Ed. (1999 –)* **2007**, *119*, 1716.
13. Mangialasche, F.; Solomon, A.; Winblad, B.; Mecocci, P.; Kivipelto, M. *Lancet Neurol.* **2010**, *9*, 702.
14. Giacobini, E. *Ann. N.Y. Acad. Sci.* **2006**, *920*, 321.
15. Dawson, R. M. *Neurosci. Lett.* **1990**, *118*, 85.
16. Bar-On, P.; Millard, C. B.; Harel, M.; Dvir, H.; Enz, A.; Sussman, J. L.; Silman, I. *Biochemistry* **2002**, *41*, 3555.
17. Zheng, H.; Youdim, M. B. H.; Fridkin, M. *ACS Chem. Biol.* **2010**, *5*, 603.
18. Telpoukhovskaia, M. A.; Patrick, B. O.; Rodríguez-Rodríguez, C.; Orvig, C. *Mol. Biosyst.* **2013**, *9*, 792.
19. Perez, C.; Daniel, K. B.; Cohen, S. M. *ChemMedChem* **2013**, *8*, 1662.
20. Leeson, P. *Nature* **2012**, *481*, 455.
21. Clark, D. E.; Pickett, S. D. *Drug Discovery Today* **2000**, *5*, 49.
22. Rishton, G. M. *Drug Discovery Today* **1997**, *2*, 382.
23. Berg, L.; Andersson, C. D.; Artursson, E.; Hörnberg, A.; Tunemalm, A.-K.; Linusson, A.; Ekström, F. *PLoS One* **2011**, *6*, e26039.
24. Bajda, M.; Więckowska, A.; Hebda, M.; Guzior, N.; Sotriffer, C. A.; Malawska, B. *Int. J. Mol. Sci.* **2013**, *14*, 5608.
25. Kochi, A.; Eckroat, T. J.; Green, K. D.; Mayhoub, A. S.; Lim, M. H.; Garneau-Tsodikova, S. *Chem. Sci.* **2013**, *4*, 4137.
26. Luo, W.; Li, Y.-P.; Tan, J.-H.; Gu, L.-Q.; Huang, Z.-S. *J. Enzyme Inhib. Med. Chem.* **2011**, *26*, 706.